The impact of strain on GeV color centers in diamond.

Thijs van Wijk[1,2], E. Aylin Melan[1,2], Emerick Y. Guillaume[1,2], & Danny E. P. Vanpoucke[1,2]

[1] QuATOMs, Hasselt University, Agoralaan Gebouw D, 3590 Diepenbeek, Belgium
[2] Institute for Materials Research (IMO), IMOMEC, IMEC vzw, Diepenbeek, Belgium

Introduction

Diamond color centers are considered excellent candidates for applications in quantum information processing, biosensors, and magnetometry.[1,2,3] Although the NV^- center is the most researched color center in diamond, the GeV center has the potential of being a superior candidate as a quantum emitter.

Interest in the GeV center and other group IV elements like SiV arises mainly from their intense zero-phonon line and small phonon sideband.[2,3] Despite a strong resemblance between the GeV center and the SiV center, GeV exhibits higher quantum photoluminescence efficiency.[4] However, further research is needed for the characterization of the GeV center under experimental conditions. Ab initio calculations provide valuable insights into the electronic energy levels of the color center under varying conditions such as strain and color center concentration. In this work, we aim to elucidate the effect of strain and defect charging on the zero-phonon line (ZPL).

I. GeV color center: charge and symmetry

The GeV color center has been characterized via quantum mechanical simulations employing Density Functional Theory (DFT). Structural relaxations have been conducted on the GeV center accommodated within a 4x4x4 supercell, considering both its neutral (GeV^0) and charged (GeV^+ & GeV^-) states. This analysis confirms the anticipated D_{3d} symmetry of the GeV color center, akin to the SiV color center.

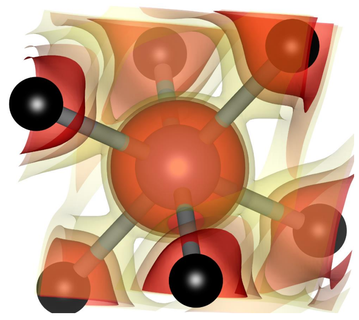

Fig I.1: *The GeV center, showing the chemical bonds between Ge and its six surrounding C atoms*

Hirshfeld-I calculations were utilized to ascertain the calculated partial charges associated with each of the defect atoms (cf. **Table I.1**.). In this context, the defect comprises the Ge atom along with its six surrounding C atoms, as depicted in **Fig I.1.** .

Charge	Ge	C
GeV^0	1.613	-0.603
GeV^+	1.710	-0.682
GeV^-	1.550	-0.549

Table I.1: *Partial charges of the Ge atom and the 6 surrounding C atoms for three different defect charges.*

Fig I.2 presents the electron density visualization at the e_g and e_g' energy levels, denoting the highest state in the valence band and the state situated within the bandgap of diamond, respectively. Visualization of these bands was conducted on the neutral GeV^0 system. A static, gamma-only calculation was performed at HSE level to create the wavefunctions.

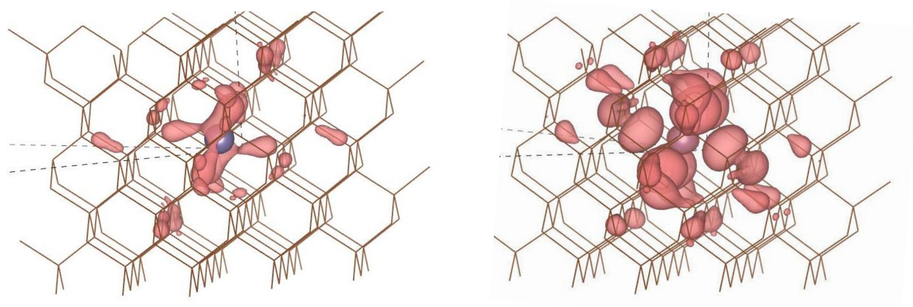

Fig I.2: *Visualization of electron density at the (a) e_g and (b) e_g' energy levels within the 4x4x4 supercell system. Computational modeling involved relaxation with the PBE functional using a 2x2x2 k-point set, followed by a static, gamma-only calculation at HSE level.*

II. Effect of strain on ZPL

The impact of strain on the ZPL of GeV centers within the diamond lattice was analyzed. This encompasses calculated ZPL energies across various supercell configurations**.** These supercell configurations correspond to different concentrations, ranging from approximately 1.5% (using a 2×2×2 conventional supercell) to 0.1% (5×5×5 conventional supercell). The effect of supercell size is shown in **Table II.1.**

Equilibrium ZPL-energy (eV)	Spin up	Spin down
222 supercell	2.178	2.493
333 supercell	1.124	1.504
444 supercell	1.341	1.748
555 supercell	1.228	1.920

Table II.1: *ZPL-energy for the equilibrium state for different supercell sizes. These DFT calculations were performed with PBE functional, using a 5x5x5 k-point set for 222 and 333 supercell and a 3x3x3 k-point set for the 444 and 555 system.*

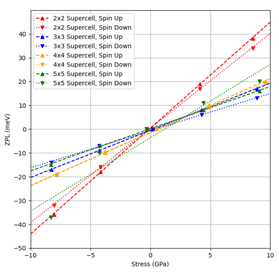

Fig II.1: *ZPL-Energy as a function of hydrostatic stress for different supercell sizes, relative to equilibrium ZPL-energy.*

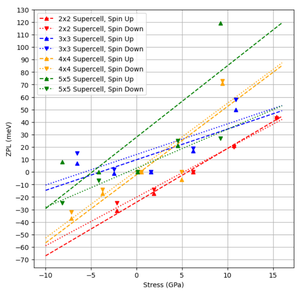

Fig II.2: *ZPL-Energy as a function of uniaxial stress for different supercell sizes, relative to equilibrium ZPL-energy.*

Two types of strain are explored: hydrostatic strain, where the cubic shape of the diamond cell is maintained, and uniaxial strain along the <100> orientation. The results are shown in **Fig II.1** and **II.2**. This research holds significance for understanding the effects of experimental strain conditions on the orientation of GeV centers within the lattice.

III. Effect of strain on energy levels

The effect of the strain on the energy levels was studied. Contradictory to the simple theoretical model where the GeV center has only five levels, DFT calculations on supercells generate the levels of the bulk diamond lattice as well. By analyzing the partial contribution of the color center atoms to a certain energy band, it was possible to reproduce the same bands as the theoretical model. **Fig III.1 a.** shows the energy levels of the unstrained crystal for the 5x5x5 supercell. **Fig III.1 b.** and **c.** contain the energy bands after a hydrostatic strain. Here, it is clear that the values of the energy levels change, but the structure itself is maintained. **Fig III.2** shows the effect of linear strain. It is visible that the degenerated energy levels will be pulled apart because the cubic symmetry of the crystal is broken. This also causes the states to mix with the bulk states of diamond. **Fig III.3 a.** and **b.** show how these energy levels look in practice, and how they can be found using the partial contribution of the atoms to the bands.

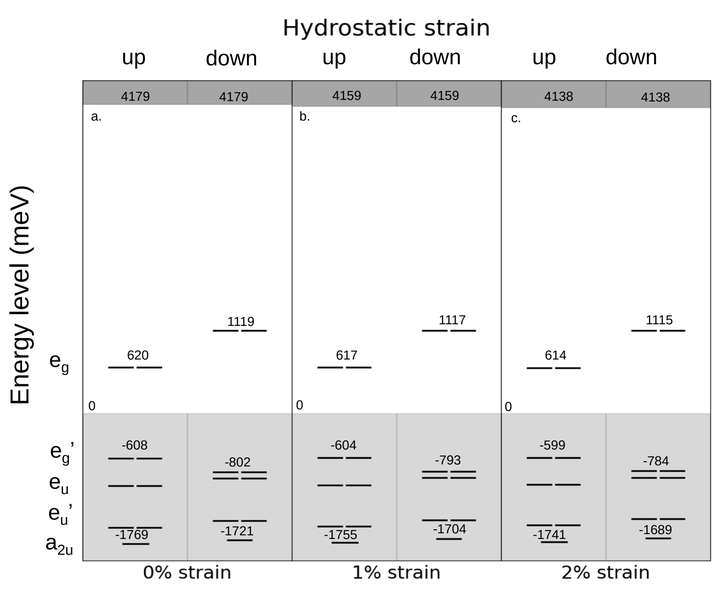

Fig III.1: *Energy levels of the GeV center for three different strains along the <111> direction (hydrostatic). Figure a. shows the equilibrium, b. and c. 1% and 2% strain.*

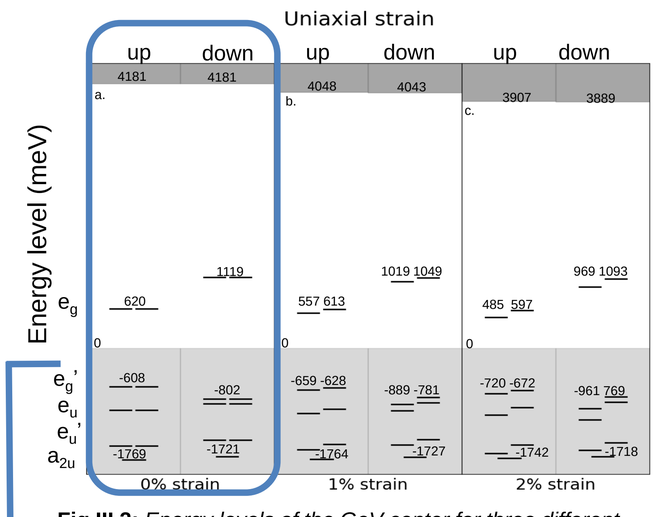

Fig III.2: *Energy levels of the GeV center for three different strains along the <100> direction (uniaxial). Figure a. shows the equilibrium, b. and c. 1% and 2% strain.*

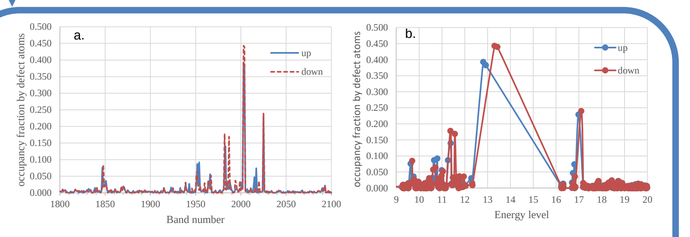

Fig III.3: *Partial contribution of GeV atoms to the energy bands. On a) the relative contribution as a function of the band number, and on b) as a function of the energy. This is used to build* **Fig III.3a.**

References:

1. D.E.P. Vanpoucke, et al. Diam. Relat. Mater. 94, (2019) 233-241.
2. K.N. Boldyrev, et al. Diam. Relat. Mater. 126, (2022) 109049.
3. G. Thiering & A. Gali, Semicond. Semimet. 103, (2020) 1-36.
4. X. Tan, et al. Surface Science. 715, (2022), 121950.